



HAL
open science

Silicon-Containing Neuropeptide Analogues as Radiopharmaceuticals for NTS 1 -Positive Tumors Imaging

Roberto Fanelli, Adrien Chastel, Santo Previti, Elif Hindié, Delphine Vimont, Paolo Zanotti-Fregonara, Philippe Fernandez, Philippe Garrigue, Frédéric Lamare, Romain Schollhammer, et al.

► **To cite this version:**

Roberto Fanelli, Adrien Chastel, Santo Previti, Elif Hindié, Delphine Vimont, et al.. Silicon-Containing Neuropeptide Analogues as Radiopharmaceuticals for NTS 1 -Positive Tumors Imaging. *Bioconjugate Chemistry*, 2020, 31 (10), pp.2339-2349. 10.1021/acs.bioconjchem.0c00419 . hal-03169750

HAL Id: hal-03169750

<https://hal.inrae.fr/hal-03169750>

Submitted on 17 May 2021

HAL is a multi-disciplinary open access archive for the deposit and dissemination of scientific research documents, whether they are published or not. The documents may come from teaching and research institutions in France or abroad, or from public or private research centers.

L'archive ouverte pluridisciplinaire **HAL**, est destinée au dépôt et à la diffusion de documents scientifiques de niveau recherche, publiés ou non, émanant des établissements d'enseignement et de recherche français ou étrangers, des laboratoires publics ou privés.

Silicon-Containing Neurotensin Analogues as Radiopharmaceuticals for NTS₁-Positive Tumors

Imaging

Roberto Fanelli,[§] Adrien Chastel,^{¥,ψ} Santo Previti,[§] Elif Hindié,^{¥,ψ} Delphine Vimont,[¥] Paolo Zanotti-Fregonara,[‡] Philippe Fernandez,^{¥,ψ} Philippe Garrigue,^{‡,‡} Frédéric Lamare,^{¥,ψ} Romain Schollhammer,^{¥,ψ} Laure Balasse,[‡] Benjamin Guillet,^{‡,‡} Emmanuelle Rémond,[§] Clément Morgat,^{¥,ψ,*‡} Florine Cavalier,^{§,*‡}

[§]*Institut des Biomolécules Max Mousseron, IBMM, UMR-5247, CNRS, Université de Montpellier, ENSCM, Place Eugène Bataillon, 34095 Montpellier cedex 5, France.*

[¥]*Univ. Bordeaux, CNRS, EPHE, INCIA, UMR 5287, F-33000 Bordeaux, France.*

^ψ*Nuclear Medicine Department, University Hospital of Bordeaux, F-33000 Bordeaux, France.*

[‡]*Houston Methodist Research Institute, Houston, TX, 77030, USA.*

[‡]*Aix-Marseille University, INSERM, Institut National de la Recherche Agronomique, Centre de Recherche en Cardiovasculaire et Nutrition, 13385 Marseille, France.*

[‡]*Aix-Marseille University, Centre Européen de Recherche en Imagerie Médicale, 13005 Marseille, France.*

[‡]These authors contributed equally.

Corresponding authors: Dr Florine Cavalier, Institut des Biomolécules Max Mousseron, IBMM, UMR-5247, CNRS, Université de Montpellier, ENSCM, Place Eugène Bataillon, 34095 Montpellier, France. ORCID: 0000-0001-5308-6416. Dr Clément Morgat, University Hospital of Bordeaux, Nuclear Medicine Department, Place Amélie Raba Léon, 33000 Bordeaux, France. ORCID: 0000-0002-9432-9223.

ABSTRACT

Purpose: Several independent studies have demonstrated the overexpression of NTS₁ in various malignancies making this receptor of interest for imaging and therapy. To date, radiolabeled neurotensin analogues suffer from low plasmatic stability and thus insufficient availability for high uptake in tumors. We report the development of ⁶⁸Ga-radiolabeled neurotensin analogues with improved radiopharmaceutical properties through the introduction of the silicon-containing amino acid trimethylsilylalanine (TMSAla). Among the series of novel radiolabeled neurotensin analogues, Ga-JMV6659 exhibits high hydrophilicity ($\log D_{7.4} = -3.41 \pm 0.14$), affinity in the low nanomolar range towards NTS₁ ($K_d = 6.29 \pm 1.37$ nM), good selectivity ($K_d \text{ NTS}_1 / K_d \text{ NTS}_2 = 35.9$) and high NTS₁-mediated internalization. It has lower efflux and prolonged plasmatic half-life in human plasma compared to the reference compound (Ga-JMV6661 bearing the minimum active fragment of neurotensin and the same linker and chelate than other analogues). In nude mice bearing HT-29 xenograft, [⁶⁸Ga]Ga-JMV6659 uptake reached $7.8 \pm 0.54\%$ ID/g 2h post-injection. Uptake was decreased to $1.38 \pm 0.71\%$ ID/g with injection of excess non-radioactive neurotensin. Radiation dose as extrapolated to human was estimated as 2.35 ± 0.6 mSv for a standard injected activity of 100MBq. [⁶⁸Ga]Ga-JMV6659 was identified as a promising lead compound suitable for PET imaging of NTS₁-expressing tumors.

Key words: neurotensin, NTS₁, PET imaging, silicon-containing amino acids, peptide, silyl side chain, cancer, ⁶⁸Ga.

INTRODUCTION

Neurotensin (NT) is an endogenous 13-amino acids peptide distributed in the central nervous system (CNS) and in peripheral tissues.¹ NT shows a wide range of biological activities: in the brain, it is involved in the dopaminergic system modulation, hypothermia and analgesia, while in periphery it modulates digestive and cardiovascular functions and proinflammatory responses.²⁻³ NT effects occur via the activation of the neurotensin receptors NTS₁ and NTS₂, belonging to the GPCR family, and NTS₃, a receptor with single transmembrane domain.⁴ The natural ligand NT has high affinity and specificity to these receptors and it has been demonstrated that the shortest active sequence is the fragment NT[8-13] (Figure 1).⁵ Several independent studies demonstrated the overexpression of NTS₁ in a panel of tumors, such as pancreatic adenocarcinoma, non-small cell lung cancer, invasive ductal breast carcinoma and prostate cancer among others.⁶⁻⁹ Interestingly, the NT/NTS₁ system is today highlighted as a pro-oncogenic factor in many tumors.¹⁰⁻¹² Consequently, NT represents a peptide of choice to develop tumors targeting vectors for the elaboration of diagnostic and therapeutic agents. However, the high sensitivity of NT to peptidases, that should be countered while preserving the fast pharmacokinetics and high tumor uptake necessary for imaging procedures, make the design of peptide analogues challenging. Neurotensin stabilization techniques account for reduction or *N*-methylation of amide bonds in [⁶⁸Ga]Ga-DOTA-NT20.3,¹³ amino acids substitutions in [⁶⁸Ga]Ga-(8),¹⁴ or replacement of amide bonds with enzymatically stable 1,2,3 triazoles in [¹⁷⁷Lu]Lu-NT-VI or IX.¹⁵ Despite, excellent *in vitro* behaviors of the stabilized peptide compounds, novel artifices are required to also improve tumor uptake.¹⁶ Some authors used a radically different strategy based on the compound SR142948A (Figure 1), bearing an adamantane moiety and known as a potent NTS₁ antagonist, leading to 3BP-227, which was elongated with a DOTA chelator for radiolabeling with ¹⁷⁷Lu.¹⁷ As a non-peptide compound, it is intrinsically resistant to proteases but exhibits much slower pharmacokinetics not suitable for PET imaging with short-lived positron-emitters like ⁶⁸Ga.

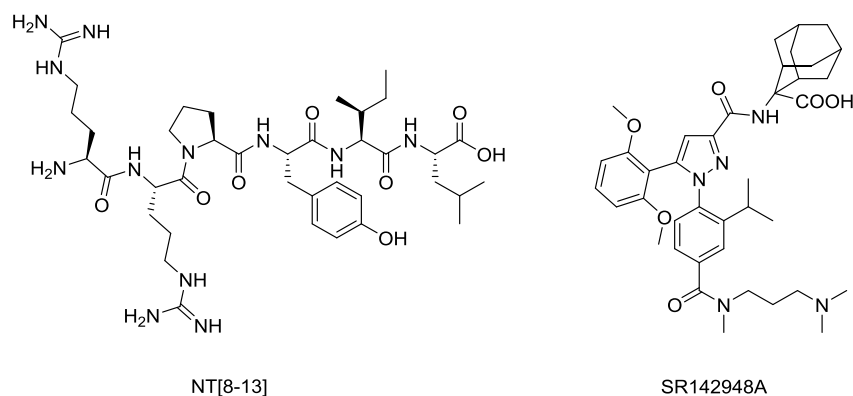


Fig. 1. NT[8-13] and SR142948A chemical structures.

In this work, our strategy has been to base our efforts on peptide neurotensin analogues, which retain high affinity and selectivity to NTS₁, high tumor uptake and exhibit fast kinetics suitable for clinical procedures.

Engineered peptides often feature improved biological properties.¹⁸ For example, introduction of unnatural amino acids brings resistance to proteolysis, while allowing the modulation of physico-chemical properties thanks to the wide variety of side chains.¹⁹⁻²⁰ Silicon/Carbon switch is reported in drug design to provide lipophilicity when carbon atom is replaced with silicon: only with this difference, logD values are slightly higher in silicon-containing derivatives.²¹⁻²⁴ Incorporation of silicon-containing amino acids in bioactive peptides,²⁵⁻³⁰ as we already reported for NT[8-13], increases both binding affinity and resistance towards enzyme degradation.³¹⁻³²

Herein, we describe the synthesis of bioconjugates based on stabilized NT[8-13] analogues radiolabeled with ⁶⁸Ga using a DOTA macrocycle complex chelator. The full characterization of this series allowed us to select a lead compound as promising radiopharmaceutical for NTS₁-positive tumors imaging.

RESULTS

Chemical synthesis of NT-conjugates. All NT analogues prepared in this study were linked to DOTA as radionuclide chelator through the amino piperidin-1-yl-acetic acid ((4)-APAc) attached to the N-terminal amine of the peptide fragment (Figure 2).

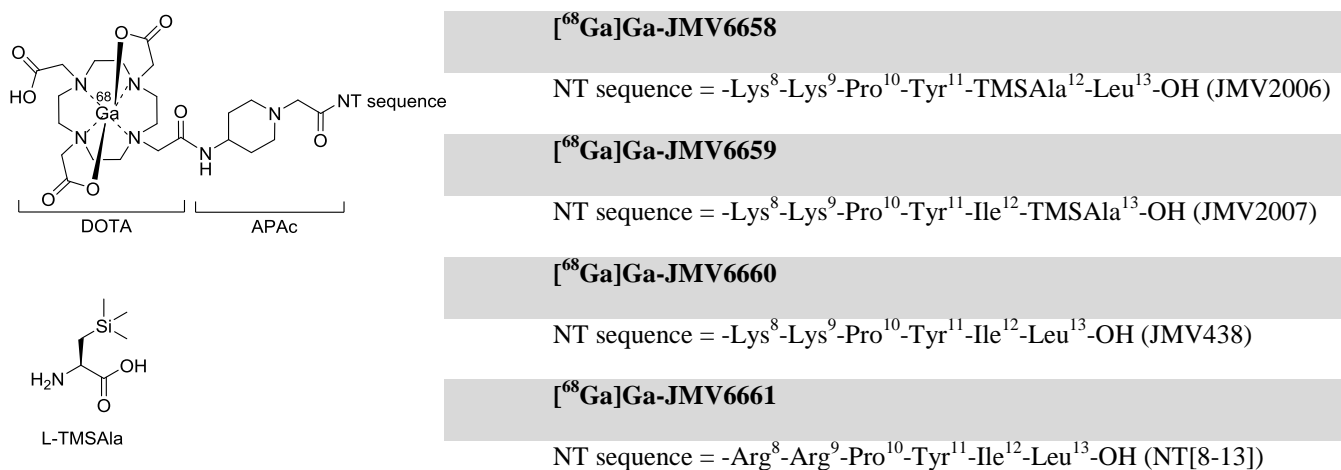


Fig. 2. Chemical structure of NT conjugates and the unnatural amino acid L-TMSAla used in this study

All NT analogues prepared in this study were linked to DOTA as radionuclide chelator through the linker amino piperidin-1-yl-acetic acid ((4)-APAc) attached to the N-terminal amine of the peptide fragment (Figure 2).

The linker APAC and the protected chelator DOTA(*t*Bu)₃-OH were consecutively coupled to the peptide. The reference compound JMV6661 was built with NT[8-13]. JMV6660 is correlated to hexapeptide JMV438 (H-Lys-Lys-Pro-Tyr-Ile-Leu-OH)³² (Figure 2), in which the two Arg residues in positions 8 and 9 have been replaced by Lys. As known, this double substitution is well tolerated in terms of binding³³⁻³⁴ and facilitates the synthesis. JMV6658 and JMV6659 contain both these two Lys residues and also include the unnatural amino acid (L)-trimethylsilylalanine (TMSAla, Figure 2) in positions 12 and 13, respectively. Fmoc-TMSAla-OH was prepared on a large scale in very good overall yield (58%, 5 steps) with 98% enantiomeric excess, using hydroxy-pinane-3-one as chiral inductor as previously reported.³⁵

To prepare the conjugates, two different strategies were considered depending on the sequence: (i) automatic solid phase peptide synthesis (SPPS) was adopted for basic sequences, while (ii) manual SPPS was preferred when using the non-commercially available amino acid TMSAla. When TMSAla was located at the C-terminal position, solution phase synthesis was initially performed, since the anchorage of Fmoc-TMSAla-OH on Wang resin failed. However, despite the steric hindrance, Fmoc-TMSAla-OH was successfully attached to 2-chlorotrityl resin, with a good loading (0.8 mmol/g) using only 1 eq. of Fmoc-TMSAla-OH to perform JMV6659 synthesis efficiently. When using this solid support, this strategy led to higher yields and purity as expected (>80% and >95%, respectively). For JMV6658 the manual strategy starting from commercially available Leu-preloaded Wang resin allowed us to monitor and stir the coupling reaction up to the completion of it. All four peptides were obtained in satisfactory yields and further purified on preparative HPLC (Table S1).

⁶⁸Ga-radiolabeling and *in vitro* studies. All compounds were radiolabeled with ⁶⁸Ga with 60% yield, high radiochemical purity (> 95% after purification), high volumic activity of 100MBq/mL and high apparent molar activity of 12.5 ± 1.3 GBq/μmol. Representative radio-HPLC and radioTLC chromatograms are available in Fig S1 and Fig S2. Radiochemical purity was stable (≥ 95%) in PBS (Fig S3) and no ⁶⁸Ga-transchelation was seen in human plasma up to 45 min (Fig S4). On RP-HPLC, relative retention times (normalized from the front solvent) were 3.17 ± 0.14 for [⁶⁸Ga]Ga-JMV6658, 3.07 ± 0.21 for [⁶⁸Ga]Ga-JMV6659, 2.99 ± 0.01 for [⁶⁸Ga]Ga-JMV6660 and 3.01 ± 0.09 for [⁶⁸Ga]Ga-JMV6661. We also looked at hydrophilicity of the ⁶⁸Ga-compounds using the PBS-octanol partition method. All radiolabeled analogues were highly hydrophilic with subtle differences. As expected, [⁶⁸Ga]Ga-JMV6658 and [⁶⁸Ga]Ga-JMV6659, bearing silicon-containing amino acids, exhibit statistically significantly higher lipophilicity *p* < 0.05 (Table 2) leading to slightly higher retention times on RP-HPLC.

NTS₁ and NTS₂ expression on HT-29 cells. Western Blot performed on HT-29 lysates showed a single band of 55kDa at the expected molecular weight of NTS₁ and a band at 45kDa corresponding to the molecular weight of NTS₂ (Figure 3A) NTS₁ and NTS₂ expressions were further confirmed by immunofluorescence. NTS₁ labeling was granular mainly located in the cytoplasm with localized reinforcements at the plasma membrane. NTS₂ labeling showed preferential staining at the plasma membrane (Figure 3 B and C).

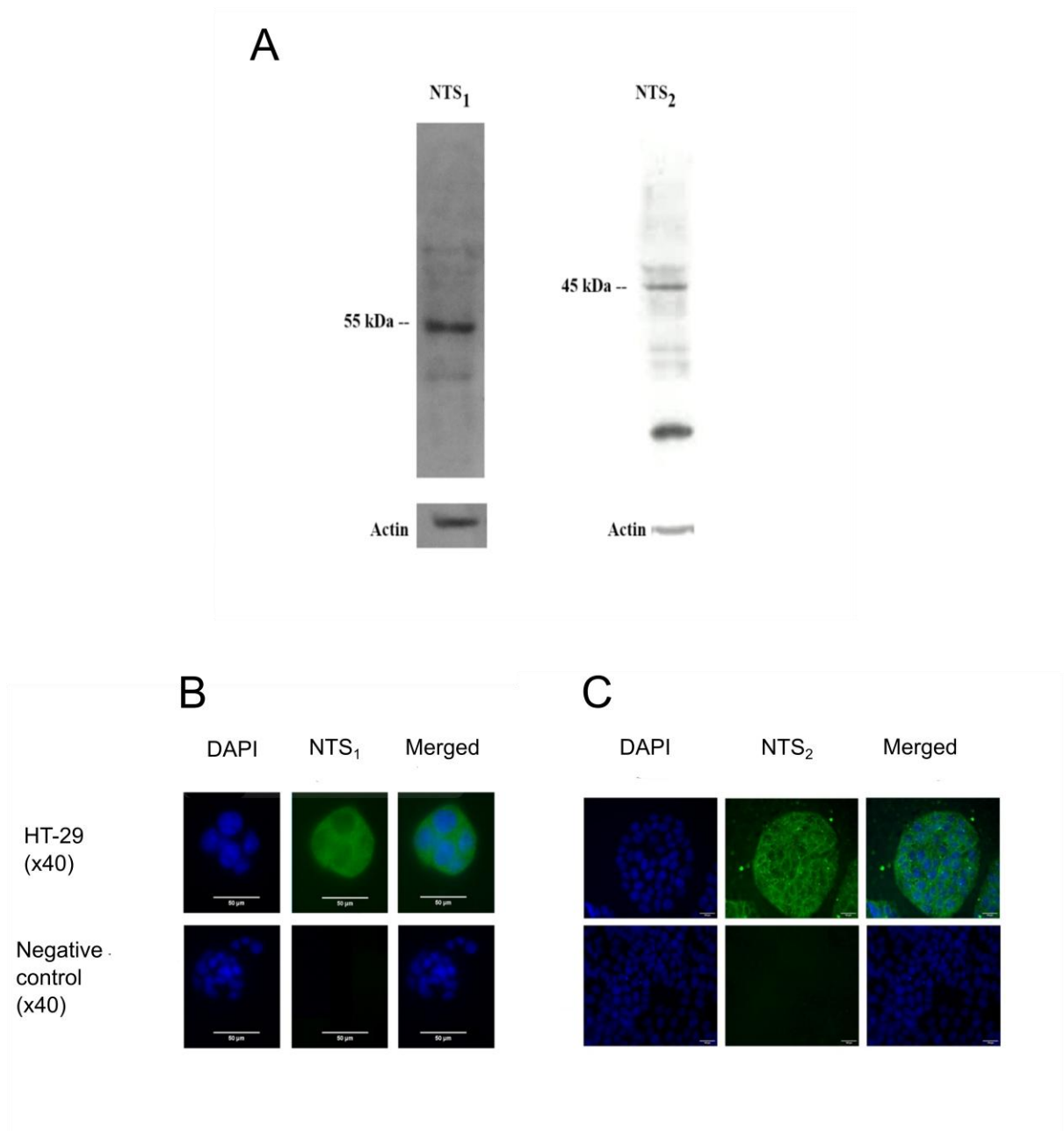


Fig. 3. (A) Representative western blots of NTS₁ and NTS₂ in HT-29 cells. Immunofluorescence of NTS₁ (B) and NTS₂ (C) in HT-29 cells. Negative controls correspond to HT-29 cells without the primary antibody. Images were obtained at 40x magnification

Binding affinity of non-labeled and ⁶⁸Ga-labeled conjugates. The ability of our series of four non-metalated conjugates to inhibit the binding of [¹²⁵I]I-Tyr³-NT (K_d = 0.22nM) on human recombinant CHO cells transfected with human NTS₁ showed that the conjugate JMV6659 is the most potent compound to NTS₁ receptor in this series with IC₅₀ = 34.5 ± 1.4 nM. Other conjugates do not retain significant NTS₁ affinity (Table 1). K_d values were next determined for the ⁶⁸Ga-labeled conjugates. Similarly, [⁶⁸Ga]Ga-JMV6659 displayed the highest NTS₁ affinity among the four analogues investigated, with a K_d value of 6.29 ± 1.37 nM towards the NTS₁ (Table 1).

TABLE 1 Binding affinity of non metalated and ⁶⁸Ga-labeled analogues

Analogues	Affinity towards NTS ₁ (nM)	Selectivity NTS ₁ /NTS ₂
JMV6658	4877 ± 1173 (IC ₅₀)	n.d
[⁶⁸ Ga]Ga-JMV6658	> 1000 (K _D)	n.a
JMV6659	34.5 ± 1.4 (IC ₅₀)	n.d
[⁶⁸ Ga]Ga-JMV6659	6.29 ± 1.37 (K _D)	35.9
JMV6660	1919 ± 1253 (IC ₅₀)	n.d
[⁶⁸ Ga]Ga-JMV6660	246.5 ± 75.39 (K _D)	0.2
JMV6661	540.5 ± 129 (IC ₅₀)	n.d
[⁶⁸ Ga]Ga-JMV6661	83.26 ± 22.49 (K _D)	> 12

n.d: not determined; n.a: not applicable

Cellular studies. Specific internalization and efflux of this series of ⁶⁸Ga-neurotensin analogues was investigated in HT-29 cells. All analogues were highly internalized (>60%, which correspond to 0.5-1% of applied dose) exception made of [⁶⁸Ga]Ga-JMV6658 (Figure 4A). As additional experiments, we also investigated potential NTS₂-mediated internalization or membrane binding of [⁶⁸Ga]Ga-JMV6659 due to the NTS₂ affinity around 0.2 μM. We observed a transient and weak NTS₂-mediated internalization of 9.0 ± 3.8% and 10.5 ± 0.7% at 10 min and 30 min respectively. At 60 min, NTS₂-mediated internalization decreased below 5%. NTS₂-membrane binding of [⁶⁸Ga]Ga-JMV6659 was < 5% at any time points (Table 4). After being internalized, efflux of the radiopeptides was also studied. [⁶⁸Ga]Ga-JMV6660 and [⁶⁸Ga]Ga-JMV6661 demonstrated high efflux (>60%) at 45 min while [⁶⁸Ga]Ga-JMV6659 exhibited significantly lower efflux than the reference compound at all time points (p<0.05)(Figure 4B).

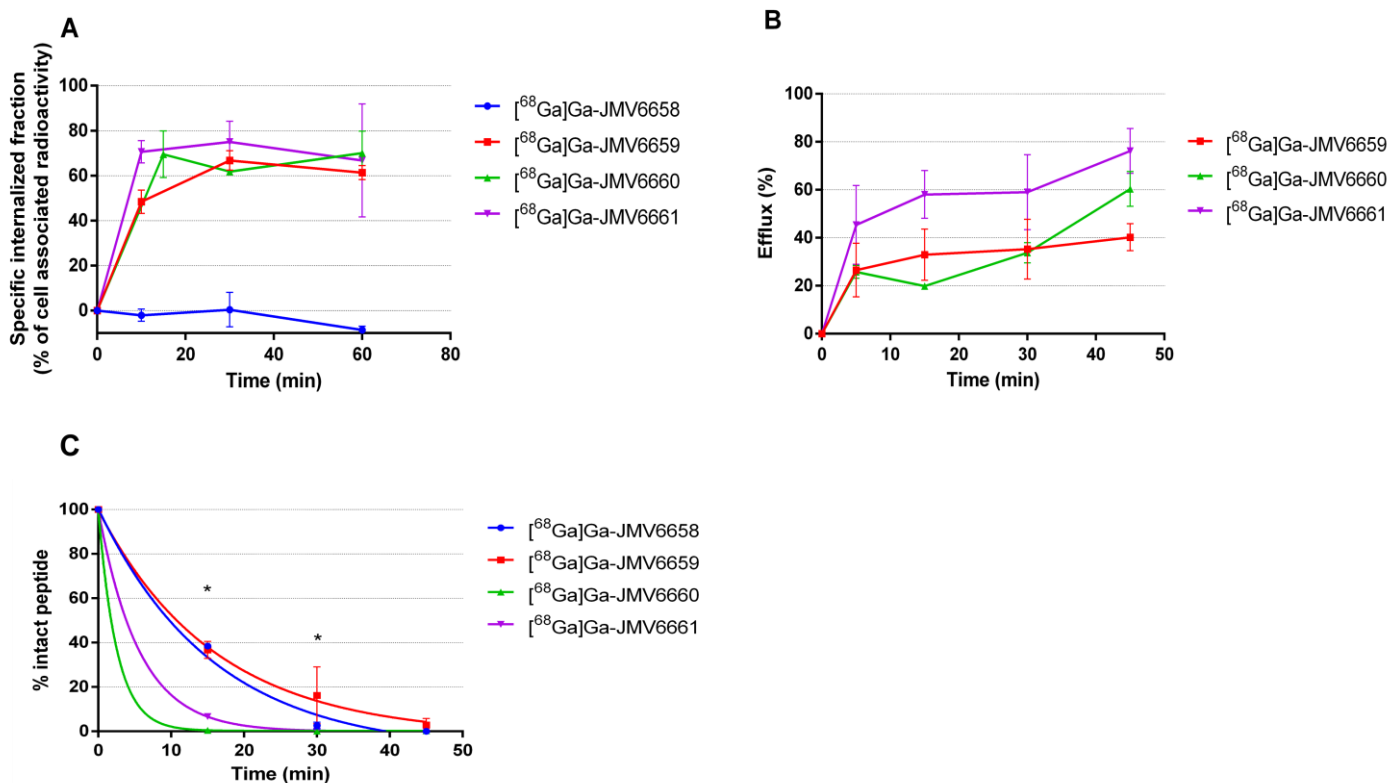


Fig. 4. Internalization (A), efflux (B) and blood plasma stability (C) of the series of radiolabeled neurotensin analogues investigated in this work. * indicates a significant difference ($p < 0.05$). At 15 minutes, [⁶⁸Ga]Ga-JMV6658 and [⁶⁸Ga]Ga-JMV6659 exhibit significantly higher blood plasma stability than [⁶⁸Ga]Ga-JMV6661. At 30 minutes, only [⁶⁸Ga]Ga-JMV6659 showed increased stability compared to the reference compound [⁶⁸Ga]Ga-JMV6661. For better clarity statistical analysis of internalization and efflux is not figured out.

Blood plasma stability. ⁶⁸Ga-neurotensin analogues were investigated in human plasma to determine their blood plasma stability. Interestingly, [⁶⁸Ga]Ga-JMV6658 and [⁶⁸Ga]Ga-JMV6659, bearing the TMSAla amino acid, retain significantly higher stability than the reference compound [⁶⁸Ga]Ga-JMV6661 at 15 minutes. At 30 minutes, only [⁶⁸Ga]Ga-JMV6659 showed increased stability compared to the reference compound. At 45 minutes, all radiolabeled neurotensin analogues were metabolized (Figure 4C). No significant differences were seen between the [⁶⁸Ga]Ga-JMV6660 and the reference compound ($p > 0.05$) at any time. After curve fitting, the 95% confidence interval (95%CI) of [⁶⁸Ga]Ga-JMV6659 half-life was [7.17 – 24.63] minutes compared to the [3.71 – 4.02] minutes 95%CI of the reference compound [⁶⁸Ga]Ga-JMV6661 (Table 2).

TABLE 2. Summary of *in vitro* radiopharmaceutical properties of a series of novel neurotensin conjugates

Analogues	LogD	95%CI of blood plasma half-life (min)	NTS ₁ -internalized fraction (% , 1h)	NTS ₁ -membrane bound fraction (% , 1h)	Efflux (% of internalized, 45min)
-----------	------	---------------------------------------	--	--	-----------------------------------

[⁶⁸ Ga]Ga-JMV6658	-3.21 ± 0.43	[7.36 – 21.61]	< 5	< 5	nr
[⁶⁸ Ga]Ga-JMV6659	-3.41 ± 0.14	[7.17 – 24.63]	61.3 ± 2.4	12.5 ± 7.3	39.4 ± 5.7
[⁶⁸ Ga]Ga-JMV6660	-3.66 ± 0.06	[1.21 – 3.28]	70.1 ± 9.7	24.7 ± 9.4	60.4 ± 7.3
[⁶⁸ Ga]Ga-JMV6661	-3.77 ± 0.38	[3.71 – 4.02]	66.8 ± 25.1	16.7 ± 4.8	76.2 ± 9.3

nr = not reported

Preclinical PET/CT imaging, biodistribution and dosimetry analysis.

For animal studies, [⁶⁸Ga]Ga-JMV6659 was used at a volumic activity greater than 700MBq/mL, RCP >97% and formulated in 30% EtOH (50μL, ~0.71μg injected). After injection of [⁶⁸Ga]Ga-JMV6659 in nude mice bearing HT-29 tumor, whole-body dynamic μPET/CT imaging clearly showed an early uptake in HT-29 tumor of 2.82 ± 1.58 %ID/g at 3 minutes (Figure 5D and Table S2). Maximum uptake of 4.35 ± 2.15 %ID/g was reached 40min after injection and remain roughly constant over-time (at 2h, uptake was 3.67 ± 1.90 %ID/g). Elimination of the radiotracer was urinary-exclusive (Figure 5 A, B and C). On biodistribution experiments, a high uptake of 7.8 ± 0.54%ID/g at 2 hours in tumor was also seen, Figure 5C and Table S2. Analysis of PET images and ex vivo biodistribution showed strong significant positive correlation (Spearman coefficient $r = 0.883$, $p=0.008$).

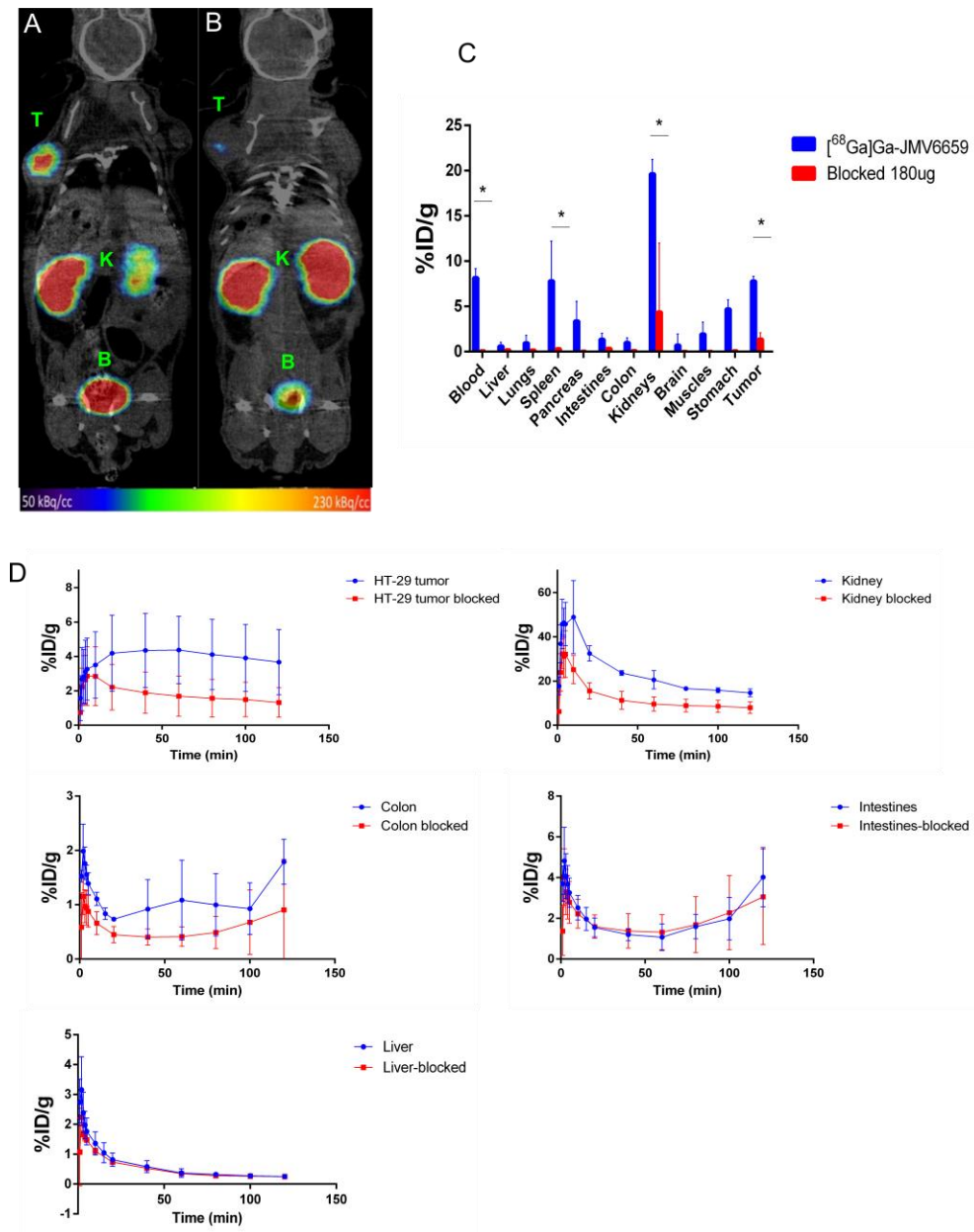


Fig. 5 μ PET/CT imaging, biodistribution and image-derived time-activity curves of $[^{68}\text{Ga}]\text{Ga-JMV6659}$ in HT-29 tumor-bearing nude mice. **A:** Fused coronal PET/CT image at 2h post-injection of a nude mice injected with $[^{68}\text{Ga}]\text{Ga-JMV6659}$ alone. **B:** Fused coronal PET/CT image at 2h post-injection of a nude mice injected with $[^{68}\text{Ga}]\text{Ga-JMV6659}$ and excess of neurotensin (180 μg) demonstrating specificity of NTS_1 targeting. T indicates the HT-29 tumor, K stands for kidneys and B means bladder. **C:** Biodistribution after animal sacrifice 2h after injection. A group of three mice received only $[^{68}\text{Ga}]\text{Ga-JMV6659}$ ($[^{68}\text{Ga}]\text{Ga-JMV6659}$ group) while the blocked group of 3 additional mice was pre-injected with 180 μg of neurotensin. **D:** PET image-derived time-activity curves (TACs) in HT-29 tumor, kidney, colon and intestines and liver.

Specificity of [^{68}Ga]Ga-JMV6659 was demonstrated by pre-injection of excess of 180 μg of neurotensin, resulting in significant lower uptake in tumor both on PET images ($p < 0.01$) and *ex vivo* biodistribution compared to the unblocked experiment (Table S2). Interestingly, blood, kidneys and spleen showed also NTS $_1$ -mediated uptake on biodistribution experiments (8.18 ± 1.00 ; 19.63 ± 1.57 ; 7.83 ± 4.39 %ID/g for the unblock group vs 0.09 ± 0.02 , 4.39 ± 7.60 , 0.33 ± 0.12 , after blocking with 180 μg of neurotensin, respectively; Table S2). On PET images, a similar pattern of NTS $_1$ -uptake was seen on kidneys at 2h after injection (Table S2, Figure 5D). Spleen exhibited also a high uptake on PET images, reaching 7.89 ± 3.39 %ID/g at 40 min post-injection. However, the NTS $_1$ -mediated process was less evident on PET images possibly due to the manual delineation of CT images. To investigate more precisely the receptor-mediated uptake on spleen and blood, another group of mice was preinjected with a small dose of 50 μg of neurotensin to produce dose-response effect. Again in this group, lower uptake on spleen and blood was shown (Table S2). Clearance of [^{68}Ga]Ga-JMV6659 from other organs was fast (Figure 5D). Only colon and intestines showed a different kinetics with an increasing signal starting at 1h post-injection. It was not possible to derived TACs for blood because aorta volume is too small to provide reliable data.

Organ-absorbed doses were estimated by using OLINDA software to extrapolate to the adult phantom the mouse distribution data of [^{68}Ga]Ga-JMV6659. Table 3 summarizes the organ-absorbed doses. Among normal organs, kidneys had the highest absorbed dose ($0.121 \pm 0.135\text{mSv/MBq}$). The effective dose was estimated at 0.0235 ± 0.006 mSv/MBq.

TABLE 3. Radiation dose estimates (mGy/MBq) of [^{68}Ga]Ga-JMV6659.

Organs	Mean	SD
Adrenals	1.47E-02	9.07E-04
Brain	3.54E-03	5.10E-04
Breasts	1.15E-02	5.51E-04
Gallbladder wall	1.43E-02	2.65E-04
Lower large intestine wall	4.64E-02	1.05E-02
Small intestine	1.47E-02	3.21E-04
Stomach wall	5.60E-02	6.84E-02
Upper large intestine wall	1.44E-02	3.00E-04
Heart wall	1.35E-02	6.08E-04
Kidneys	1.21E-01	1.35E-01
Liver	6.08E-03	2.63E-03
Lungs	9.44E-03	3.31E-03
Muscle	1.27E-02	4.58E-04
Ovaries	1.48E-02	4.36E-04
Pancreas	7.79E-03	1.40E-03
Red marrow	1.08E-02	3.06E-04

Osteogenic cells	1.80E-02	7.64E-04
Skin	1.12E-02	5.03E-04
Spleen	2.29E-02	8.11E-03
Testes	1.25E-02	6.11E-04
Thymus	1.28E-02	6.00E-04
Thyroid	1.27E-02	6.56E-04
Urinary bladder wall	1.40E-02	5.69E-04
Uterus	1.45E-02	5.29E-04
Total body	1.35E-02	3.21E-04
Effective dose (mSv/MBq)	2.35E-02	6.40E-03

DISCUSSION

Targeting the NTS₁ receptor holds promise in nuclear oncology as this receptor is expressed in many tumors³⁶ and therefore offers the possibility of targeting these tumors with radiolabeled NT analogs for imaging or therapy.³⁷ Several groups have been very active at producing radiolabeled neurotensin analogues with better stability but current analogs still leave room for improvement in term of pharmacokinetics¹⁷ or tumor uptake.¹³⁻¹⁴ In this work we present a novel series of peptidic neurotensin analogues. All conjugates bear the APac linker given its ability to protonate being described as an advantage for improving affinity due to its positive charge.³⁸⁻³⁹ The JMV6660 conjugate was constructed with two lysine residues instead of arginine, given that this substitution was demonstrated to be well-tolerated in terms of binding and biological activities of the NT analogues,⁴⁰ although in our conditions the plasmatic stability was not significantly improved by the use of lysine substitution alone. Additionally, *Nε*-Boc-*Nα*-Fmoc-Lys-OH is easier to handle compared to corresponding Arg analogue, which carries Pdf or Pmc as *Nε*-protecting group. Finally, conjugates JMV6658 and JMV6659 were synthesized by replacing hydrophobic natural amino acids with the highly hydrophobic TMSAla at C-terminal position which has already proven by our research group to lead to improved NTS₁ affinity.^{32,41} Lipophilicity at the C-terminal end of the NT[8-13] is required for high affinity binding to the NTS₁ pocket. Considering the high lipophilicity of TMSA-Ala, we replaced the two positions, 12 and 13 respectively, of the lipophilic tail of NT sequence. The replacement of Leu in position 13 resulted in improved affinity.³²

After validation steps confirming NTS₁ and NTS₂ expression in HT-29 cells (Figure 3), cellular experiments were carried out. Thus, we determined affinity and selectivity of unlabeled bioconjugates and radiolabeled counterparts regarding NTS₁ (Table 1). Results from competition experiments indicate that the unlabelled bioconjugates suffer from a dramatic loss in affinity compared with their respective binding sequences³² due to the introduction of the APac linker and the DOTA macrocycle. Nevertheless, ⁶⁸Ga-bioconjugates showed an apparent improvement in affinity by a factor ~ 5 compared with their unlabeled counterparts. However, differences in the testing systems used make direct comparisons hazardous. Overall, [⁶⁸Ga]Ga-JMV6659 exhibits affinity in the nanomolar range, similarly to some

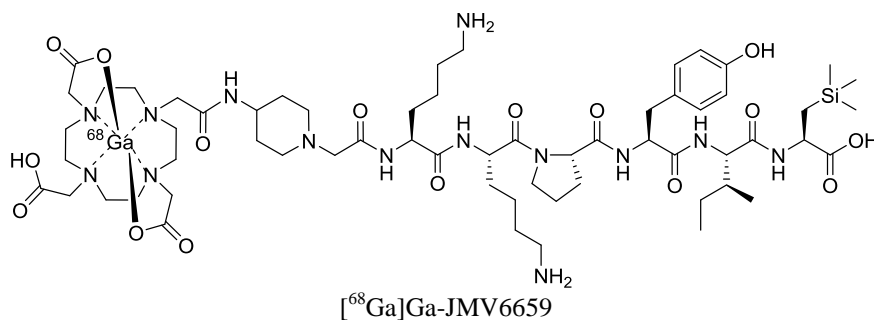
radiolabeled neurotensin analogues, but importantly shows the best affinity and selectivity among ^{68}Ga -labelled monomeric neurotensin analogues.⁴² Impact of other metallic isotopes (^{111}In , ^{177}Lu or ^{161}Tb for example) are currently being investigated.

We pursued our efforts to characterize our series by determining affinity to NTS_2 and thus selectivity to NTS_1 . [^{68}Ga]Ga-JMV6659 exhibits also good selectivity to NTS_1 receptor. We here show that [^{68}Ga]Ga-JMV6659 has the highest reported selectivity to NTS_1 (Table 1). Selectivity is unfortunately rarely investigated during radiopharmaceutical characterization of neurotensin analogues. This point is crucial since little is known regarding physiological expression of NTS_2 in periphery⁴³⁻⁴⁴ and unselective targeting may increase the background. NTS_1 -mediated internalization of [^{68}Ga]Ga-JMV6659, [^{68}Ga]Ga-JMV6660 and reference [^{68}Ga]Ga-JMV6661 was up to 60 – 70% at 1h (similar to other peptide analogues¹³⁻¹⁴), unlike [^{68}Ga]Ga-JMV6658 which did not internalize in HT-29 cells in line with its low NTS_1 affinity (Table 2, Figure 4).

Good internalization is of major importance for future targeted radionuclide therapy applications with short-range particle emitters such as metallic emitters rich in Auger electrons (^{161}Tb , $^{58\text{m}}\text{Co}$...) or α -emitters (^{225}Ac , ^{213}Bi , ^{227}Th ...).⁴⁵⁻⁴⁸ We also investigated the membrane bound fraction of our ^{68}Ga -neurotensin analogues. None of the analogues remained bound to the membrane NTS_1 (and NTS_2 for [^{68}Ga]Ga-JMV6659) in high amount revealing that all analogues might behave like agonists (antagonists do not promote Ca^{2+} release and internalization and remain located at the cell membrane).³⁶ Efflux experiments were also carried out and indicated that [^{68}Ga]Ga-JMV6660 and [^{68}Ga]Ga-JMV6661 were more released from the cells (~60 – 70%) compared to [^{68}Ga]Ga-JMV6659 (~40% efflux) (Table 2, Figure 4).

TABLE 4. Summary of radiopharmaceutical properties of lead-compound [^{68}Ga]Ga-JMV6659.

K_a (nM)	
NTS_1	NTS_2
6.29 ± 1.37	225.5 ± 34.0
Selectivity $\text{NTS}_1/\text{NTS}_2$	
35.9	
Plasmatic half-life (95% CI)	
[7.17 – 24.63] min	
LogD	
-3.41 ± 0.14	
Internalized fraction (%)	
NTS_1	NTS_2
61.3 ± 2.4	~5
Membrane-bound fraction (%)	
NTS_1	NTS_2
12.5 ± 7.3	< 5
Efflux (%)	
39.4 ± 5.7	
Binding to plasma protein (%)	
21.04 ± 3.15	



Uptake in HT-29 tumor (%ID/g at 2h)

7.8 ± 0.54

Modification at position 13 seems to be critical to also modulate cellular efflux. We are working to decipher the molecular mechanisms involved in this cellular efflux. [⁶⁸Ga]Ga-JMV6659 was then injected in mice for in vivo imaging. As expected uptake in HT-29 xenograft was high and increased over-time to reach a maximum of 7.8%ID/g at 2h on biodistribution experiments. This value is substantially higher than the uptake found with peptide neurotensin analogues reported so far and in the same range as the non-peptide antagonist [¹⁷⁷Lu]Lu-3BP-227 that has been recently used in patients.^{14,17,49} For instance, [⁶⁸Ga]Ga-(8) uptake in nude mice bearing HT-29 tumor was reported to reach a maximum 10 min after injection ($2.77 \pm 0.47\%$ ID/g) and then decrease to $1.55 \pm 0.35\%$ ID/g at 1h.¹⁴ Similarly, uptake of [⁶⁸Ga]Ga-DOTA-NT-20.3 was only detectable at 45 minutes post-injection,¹³ while we herein noted very early uptake of [⁶⁸Ga]Ga-JMV6659 which begins at 3 minutes post-injection on the μ PET/CT images, reaches its maximum at 40 min and then remains constant.

The increase of [⁶⁸Ga]Ga-JMV6659 uptake over time in the tumor reflects the higher stability of this compound compared with the reference compound. Although more stable peptide analogues have been reported in the literature,⁴² the stability should fit with the kinetics of the distribution process. Therefore, a high stability would be required for probes with long retention in blood and thus slow distribution. Indeed, our lead-compound does not showed the highest stability reported, but this value is high-enough given the early and high uptake of [⁶⁸Ga]Ga-JMV6659 in HT-29 tumor (Figure 5).

Therefore, [⁶⁸Ga]Ga-JMV6659 displays fast pharmacokinetics common with other radiopeptides⁴² as demonstrated by the distribution kinetics of the free fraction of [⁶⁸Ga]Ga-JMV6659 in NTS₁-positive organs (Figure 5). This contrasts with the slow uptake of [¹¹¹In]Lu-3BP227 in tumor cells which is 6 hours after injection.¹⁷ A ¹⁸F-labeled glycoconjugate of 3BP227 has been developed with a much faster pharmacokinetics but the uptake in HT-29 tumors was dramatically decreased to 0.74%ID/g at 1h.⁵¹ In biodistribution experiments, we also noted significant dose-response NTS₁-mediated uptake in blood, kidneys and spleen like in other previous studies.^{17,42} In the study of Schulz *et al*, the high blood uptake of [¹¹¹In]In-3BP227 was 5-fold higher in mice bearing NTS₁-positive xenograft than in NTS₁-negative xenografted mice, suggesting a receptor-mediated process. To get more insight on this binding that can be limiting for future therapeutic trials, the plasma protein binding of [⁶⁸Ga]Ga-JMV6659 was studied *ex vivo*. Results showed that the radiopeptide effectively binds to plasma proteins in a non-specific manner ($21.0 \pm 3.2\%$) (Table 4 and Table S3). This value illustrate well the ~18% fraction of [⁶⁸Ga]Ga-JMV6659 not displaced in the *in vivo* 180 μ g blocked-experiment (Figure 5) and is similar to previous works⁵² but much lower than In, Lu and Y-labeled derivatives

of the non-peptide antagonist SR142948A which showed ~90% binding on human plasma protein.⁵³ Additionally, the literature reported that human blood cells (macrophages and neutrophils) express NTS₁ as well as circulating B cells⁵⁴⁻⁵⁶ supporting the specific uptake of [⁶⁸Ga]Ga-JMV6659 in blood and by extension the spleen. Using [¹¹¹In]In-JMV6659, we found that NTS₁ and NTS₂ are presents on human neutrophils (but not on lymphocytes; data will be presented on a separate article) explaining the tumor-to-blood ratio of [⁶⁸Ga]Ga-JMV6659 ~1 at 2h, which is lower than other peptide probes developed to target NTS₁,⁴² but very similar to that observed in some patients.¹⁶ Investigation of later time points is scheduled with the ¹¹¹In-version of JMV6659. Overall, the blood uptake is a combination of two mechanisms including a specific binding to blood cells and a non-specific binding to plasma proteins. One can argue that this value may hinder clinical translation of this radiopeptide for imaging, but uptake in blood may be easily separated from that of tumor lesions thanks to the associated anatomical imaging routinely performed with PET using Computerized Tomography or Magnetic Resonance Imaging. However, the hematological toxicity of the ¹⁷⁷Lu-labeled version should be carefully studied for future therapeutic trials using high activities. In the first-in-human study performed with [¹⁷⁷Lu]Lu-3BP227, which presents similar uptake in blood than [⁶⁸Ga]Ga-JMV6659, the hematotoxicity profile looks reassuring after intravenous infusion of 5.5GBq of the radiopharmaceutical.⁴⁹ could also be the organs at risk considering the high NTS₁-mediated uptake in mice kidneys of $19.66 \pm 1.57\%ID/g$ but, for comparison, therapeutic infusion [¹⁷⁷Lu]Lu-PSMA-617 does not require kidneys protection while this radiopharmaceutical exhibits a very high and PSMA-specific uptake of $137.2 \pm 77.8\%ID/g$ in mice.⁵⁷ Given the high tumor uptake, [⁶⁸Ga]Ga-JMV6659 provides therefore a tumor-to-kidney ratio of 0.4 at 2h, similar or even better than other radiolabeled neurotensin peptides¹³⁻¹⁵ but indeed lower than non-peptide antagonists due to their hepatic clearance.^{17,58} Consequently, the tumor-to-liver ratio, which was as high as 15.45 ± 6.80 at 2h, follows the opposite pattern. The tumor-to-muscle ratio reaches 5.22 ± 2.84 at 2h and reflects the low unspecific binding of the radiopharmaceutical. Finally, [⁶⁸Ga]Ga-JMV6659 was rapidly eliminated from other organs excepted from colon and intestines which demonstrated a kind of redistribution process after 1h (Figure 5). Currently, we could not explain this phenomenom, but this was already seen with other probes targeting NTS₁ ([⁶⁸Ga]Ga-6 showed ~ 50% increase of uptake in intestines between 30 and 60min).¹⁴ Finally, we performed a radiation dosimetry estimate. This is the first estimation of human absorbed dose from radiolabeled neurotensin analogue. For a proposed median activity of 100MBq, the extrapolated radiation dose is 2.35 mSv, which is comparable to other ⁶⁸Ga-based agents used in clinics.⁵⁹⁻⁶⁰

CONCLUSION

In conclusion, we have reported a series of novel ⁶⁸Ga-radiolabeled neurotensin analogues, in which Arg⁸-Arg⁹ sequence was replaced with Lys⁸-Lys⁹ and silicon-containing amino acid (L)-trimethylsilylalanine (TMSAla) was

inserted in position 12 or 13. Interestingly, the conjugate [⁶⁸Ga]Ga-JMV6659 exhibited the highest binding affinity towards NTS₁ ($K_d = 6.29 \pm 1.37$ nM), good selectivity over NTS₂ ($K_d \text{NTS}_1 / K_d \text{NTS}_2 = 35.9$) and increased stability in human plasma with respect to the reference analogue [⁶⁸Ga]Ga-JMV6661 (> 5 folds). High NTS₁-mediated internalization, moderate efflux in cells and a very promising specific tumor uptake of $7.8 \pm 0.54\%$ ID/g at 2h in mice were also demonstrated with [⁶⁸Ga]Ga-JMV6659. The blood uptake of $8.18 \pm 1.00\%$ ID/g deserves further investigations. At the light of these data, summarized in table 34, [⁶⁸Ga]Ga-JMV6659 was identified, among this series, as the most promising radiopharmaceutical for NTS₁-targeted tumor imaging..

EXPERIMENTAL PROCEDURES

Radiochemistry.

⁶⁸Ga-radiolabeling. Radiolabeling was achieved using the FastLab automate cassette system (GE Healthcare). 1.1ml of ⁶⁸GaCl₃ (~600MBq) in HCl 0.1M (Galli Eo®, IRE-EliT, Belgium) was incubated, without further purification, with 50µg (37 – 39 nmol) of each analogue in acetate buffer (0.1M, pH4.6, final volume 2mL) and heated using microwave (GE MicroWave System 100; 100-240 Vac; 50-60Hz; 500W; Fuses 2xT6AH 250V) at 90°C for 5 minutes. The crude peptide was then purified by a Sep-Pak Light C₁₈ cartridge (WAT023501) using 0.5mL of ethanol and then formulated in PBS in order to obtain a final volume of 1.1mL. Radiochemical purity was monitored with UV-radio HPLC and TLC analysis. Full description of material used for quality control is available in Supporting information. Non-decay corrected apparent molar activities were determined by dividing the activity obtained at the end of synthesis by the amount of precursor used for radiolabeling.

Radiolabeling stability in PBS and human plasma. At each time point an aliquot (4 µL) was taken and radiochemical purity was determined by TLC analysis. The study of the radiolabeled analogues was performed at different time points (0, 15min, 30min, 45min). Experiments were performed twice in triplicates for each radiolabeled neurotensin analogues.

Biological evaluation.

Cells were obtained from the University of Bordeaux and no additional authentication was performed by the authors of this study. As validation steps, the HT-29 cells were checked regarding NTS₁ and NTS₂ expression (supplemental text). For all *in vitro* experiments, the volume of radiolabeled neurotensin analogues used was <1% of the total volume of each well.

Binding affinity of non-metallated peptide conjugates–Binding assays were performed using competition experiments as previously described.¹⁷

Stability of ⁶⁸Ga-radiolabeled neurotensin analogues in human plasma. 37MBq of each radiolabeled analogue (~0.3nmol in ~20µL) were incubated in 2mL of human plasma. At various time points (0, 15, 30 and 45 minutes), an aliquot of 50µL was taken and proteins were precipitated using 100µL ethanol. After centrifugation at 13000 rpm for 5 minutes, 50µL of the supernatant was diluted in 150µL of water and analyzed with radio-UV HPLC. Experiments were performed twice. 95%CI of plasmatic half-lives were calculated by mono-exponential fitting using GraphPad prism software (v6.01).

Hydrophilicity studies. The hydrophilicity of each radiolabeled analogue was assessed by the PBS–octanol distribution coefficient method as previously described in triplicates for three independent experiments.¹⁴

Saturation binding assay of ⁶⁸Ga-NT-conjugates. The affinity of the ⁶⁸Ga-labeled peptides was studied on HT-29 cells seeded at a density of 1 million cells per well in 6-well plates (Corning®, area of each well 9.5cm²) and incubated overnight with complete medium. Well plates were first set on ice 30 minutes before the beginning of the experiment. ⁶⁸Ga-labeled radiopeptides were then added to the medium at concentration of (0.1, 1, 10, 100, 1000nM) and cells were incubated (in triplicates) for 2 hours at 4 °C. Incubation was stopped by removing medium and washing cells twice with ice-cold PBS. Finally, cells were treated with NaOH (1M) and radioactivity was measured in a gamma counter. In order to assess for non-specific affinity, excess non-radioactive neurotensin (final concentration 1µM), or levocabastine (a selective antagonist for NTS₂, final concentration 1µM), was added to selected wells.

In vitro internalization and efflux studied studies.

HT-29 cells were cultured as described in saturation binding experiments above. Internalization and efflux experiments were performed according to published procedures¹⁴ with only minor modification (1MBq, 8-15pmol, of the respective ⁶⁸Ga-labeled radiopeptides was used and NTS₂ mediated internalization and NTS₂-membrane bound fraction of [⁶⁸Ga]Ga-JMV6659 was determined using 1µM of levocabastine). To also verify the NTS₁ specificity, blocking experiments were performed for all radiopeptides by using 1µM of neurotensin.

Small animal PET imaging and biodistribution study. Animal experiments were authorized by APAFiS #14191 on 2018/12/05 for 5 years after evaluation by the Ethics committee CE71. Animals were handled following national guidelines R.214-87 and R.214-126. HT-29 tumor-bearing mice (n=3) were injected intravenously with 4.6 ± 0.6 MBq of [^{68}Ga]Ga-JMV6659 under 2% isoflurane anesthesia. PET dynamic images were acquired for 2 hours (5×1min, 3×5min, 5 ×20min) and began 10 seconds before injection on a Nanoscan PET/CT camera (Mediso). For blocking experiments, 3 other mice were intravenously injected with an excess (180μg) of neurotensin 25 minutes before [^{68}Ga]Ga-JMV6659 injection, and PET images were acquired for 2 hours with the same dynamic acquisition protocol. A second group of 3 mice were blocked with a smaller dose of neurotensin (50μg). For biodistribution studies, mice were sacrificed after PET imaging. The tumors and other tissues (lung, liver, kidneys, brain, spleen, muscle, stomach, intestines, pancreas and colon), as well as blood, were removed and weighed. Radioactivity of the samples was measured using a γ -counter and expressed as %ID/g. Processing of reconstructed images was performed using PMOD software (version 3.5). For each mouse, the following organs: lungs, whole brain, spleen, stomach, liver, colon, tumor, kidney, intestines were manually delineated on CT images and subsequently applied to the dynamic PET image series. Data were expressed in %ID/g after normalization of standard PET value expressed in kBq/mL by the volume of the ROI, the injected activity and weight of organ measured after sacrifice. The decay-corrected mean time-activity curves (TACs) were determined for each target organ.

Radiation dose estimates.

Human radiation dosimetry estimates of [^{68}Ga]Ga-JMV6659 were calculated from mouse biodistribution data, using the MIRD methodology to calculate the internal organ radiation dose and extrapolate to humans. Briefly, the radiation dose to a given organ is:

$$D_T = \sum_S A_S DF(T \leftarrow S)$$

As stands for the cumulative activity within an internal source organ expressed in unit of Bq.s per Bq administrated and $DF(T \leftarrow S)$ are the dose factors for source organ S irradiating the target organ T. The summation is performed on all source-to-target organ combination and for every target organ in the body. The cumulative activity is obtained by integration of time-activity data for each organ (tumor, brain, lung, kidneys, stomach, spleen, liver, intestines and pancreas), and the residence time was therefore derived for each mouse organ and then extrapolated to humans using the ratio in organ weights of mouse and human. Residence time of the rest of the body was calculated by subtracting to the total residence time ($t_{1/2} \ln(2)$), the sum of organ residence times. Extrapolated human residence times were

used as input to the dosimetry software OLINDA/EXM. Absorbed doses to the organs were derived for the reference male phantom.

Statistical analyses.

All statistical analyses were performed with GraphPad Prism® software package. The unpaired student t-test was used to determine statistical significance between 2 groups. For comparison between 3 or more groups, a two-ways ANOVA with multiple comparison test correction was used. Differences at the 95% confidence level ($p < 0.05$) were considered significant.

ACKNOWLEDGEMENT

This work was partly funded by France Life Imaging (grant ANR-11-INBS-0006) from the French program «Investissements d’Avenir» and by the Institut National du Cancer (INCa PLBIO 2017, THERACAN project). This work was achieved within the context of the Laboratory of Excellence TRAIL ANR-10-LABX-57.

SUPPORTING INFORMATION AVAILABLE

Synthesis and control of peptides, characterization of NTS₁ and NTS₂ expressions in HT-29 cells, quality controls of ⁶⁸Ga-neurotensin analogues, stability of ⁶⁸Ga-radiolabeling in PBS and in human plasma, biodistribution assessed on PET images and after animal sacrifice and plasma protein binding of [⁶⁸Ga]Ga-JMV6659 are fully described in Supporting Information.

REFERENCES

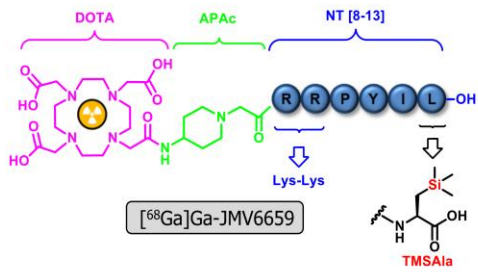
1. Carraway, R. and Leeman, S. E. (1973) The Isolation of a New Hypotensive Peptide, Neurotensin, from Bovine Hypothalami. *J Biol Chem* 248, 6854-6861.
2. St-Gelais, F., Jomphe, C. and Trudeau, L. E. (2006) The Role of Neurotensin in Central Nervous System Pathophysiology: What Is the Evidence? *J Psychiatry Neurosci* 31, 229-245.
3. Boules, M., Li, Z., Smith, K., Fredrickson, P. and Richelson, E. (2013) Diverse Roles of Neurotensin Agonists in the Central Nervous System. *Front Endocrinol* 4, 1-16.
4. Sarret, P. and Cavalier, F. (2018) Neurotensin and Its Receptors. *Neuroscience and Biobehavioral Psychology* 1-17.
5. Carraway, R. and Leeman, S. E. (1975) The Amino Acid Sequence of a Hypothalamic Peptide, Neurotensin. *J Biol Chem* 250, 1907-1911.
6. Korner, M., Waser, B., Strobel, O., Buchler, M. and Reubi, J. C. (2015) Neurotensin Receptors in Pancreatic Ductal Carcinomas. *EJNMMI Res* 5, 17-23.
7. Alifano, M., Souaze, F., Dupouy, S., Camilleri-Broet, S., Younes, M., Ahmed-Zaid, S. M., Takahashi, T., Cancellieri, A., Damiani, S., Boaron, M., et al. (2010) Neurotensin Receptor 1 Determines the Outcome of Non-Small Cell Lung Cancer. *Clin Cancer Res* 16, 4401-4410.

8. Morgat, C., Chastel, A., Molinie, V., Schollhammer, R., Macgrogan, G., Velasco, V., Malavaud, B., Fernandez, P. and Hindie, E. (2019) Neurotensin Receptor-1 Expression in Human Prostate Cancer: A Pilot Study on Primary Tumors and Lymph Node Metastases. *Int J Mol Sci* 20, 1721-1730.
9. Dupouy, S., Doan, V. K., Wu, Z., Mourra, N., Liu, J., De Wever, O., Llorca, F. P., Cayre, A., Kouchkar, A., Gompel, A. et al. (2014) Activation of EGFR, HER2 and HER3 by Neurotensin/Neurotensin Receptor 1 Renders Breast Tumors Aggressive yet Highly Responsive to Lapatinib and Metformin in Mice. *Oncotarget* 5, 8235-8251.
10. Kim, J. T., Weiss, H. L. and Evers, B. M. (2017) Diverse Expression Patterns and Tumorigenic Role of Neurotensin Signaling Components in Colorectal Cancer Cells. *Int J Oncol* 50, 2200-2206.
11. Dupouy, S., Mourra, N., Doan, V. K., Gompel, A., Alifano, M. and Forgez, P. (2011) The Potential Use of the Neurotensin High Affinity Receptor 1 as a Biomarker for Cancer Progression and as a Component of Personalized Medicine in Selective Cancers. *Biochimie* 93, 1369-1378.
12. Norris, E. J., Zhang, Q., Jones, W. D., DeStephanis, D., Sutker, A. P., Livasy, C. A., Ganapathi, R. N., Tait, D. L. and Ganapathi, M. K. (2019) Increased Expression of Neurotensin in High Grade Serous Ovarian Carcinoma with Evidence of Serous Tubal Intraepithelial Carcinoma. *J Pathol* 248, 352-362.
13. Alshoukr, F., Prignon, A., Brans, L., Jallane, A., Mendes, S., Talbot, J. N., Tourwe, D., Barbet, J. and Gruaz-Guyon, A. (2011) Novel DOTA-Neurotensin Analogues for ¹¹¹In Scintigraphy and ⁶⁸Ga PET Imaging of Neurotensin Receptor-Positive Tumors. *Bioconjug Chem* 22, 1374-1385.
14. Maschauer, S., Einsiedel, J., Hubner, H., Gmeiner, P. and Prante, O. (2016) ¹⁸F- and ⁶⁸Ga-Labeled Neurotensin Peptides for PET Imaging of Neurotensin Receptor 1. *J Med Chem* 59, 6480-6492.
15. Mascarin, A., Valverde, I. E., Vomstein, S. and Mindt, T. L. (2015) 1,2,3-Triazole Stabilized Neurotensin-Based Radiopeptidomimetics for Improved Tumor Targeting. *Bioconjug Chem* 26, 2143-2152.
16. Buchegger, F., Bonvin, F., Kosinski, M., Schaffland, A. O., Prior, J., Reubi, J. C., Blauenstein, P., Tourwe, D., Garcia Garayoa, E. and Bischof Delaloye, A. (2003) Radiolabeled Neurotensin Analog, ^{99m}Tc-NT-XI, Evaluated in Ductal Pancreatic Adenocarcinoma Patients. *J Nucl Med* 44, 1649-1654.
17. Schulz, J., Rohracker, M., Stiebler, M., Goldschmidt, J., Grosser, O. S., Osterkamp, F., Pethe, A., Reineke, U., Smerling, C. and Amthauer, H. (2016) Comparative Evaluation of the Biodistribution Profiles of a Series of Nonpeptidic Neurotensin Receptor-1 Antagonists Reveals a Promising Candidate for Theranostic Applications. *J Nucl Med* 57, 1120-1123.
18. Jackson, J. A., Hungnes, I. N., Ma, M. T. and Rivas, C. (2020) Bioconjugates of Chelators with Peptides and Proteins in Nuclear Medicine: Historical Importance, Current Innovations, and Future Challenges. *Bioconjug Chem* 31, 483-491.
19. Blaskovich, M. A. (2016) Unusual Amino Acids in Medicinal Chemistry. *J Med Chem* 59, 10807-10836.
20. Hapău, D., Rémond, E., Fanelli, R., Vivancos, M., René, A., Côté, J., Besserer-Offroy, É., Longpré, J.-M., Martinez, J., Zaharia, V. et al. (2016) Stereoselective Synthesis of β -(5-Arylthiazolyl) α -Amino Acids and Use in Neurotensin Analogues. *Eur J Org Chem* 2016, 1017-1024.
21. Fujii, S., Miyajima, Y., Masuno, H. and Kagechika, H. (2013) Increased Hydrophobicity and Estrogenic Activity of Simple Phenols with Silicon and Germanium-Containing Substituents. *J Med Chem* 56, 160-166.
22. Ramesh, R. and Reddy, D. S. (2018) Quest for Novel Chemical Entities through Incorporation of Silicon in Drug Scaffolds. *J Med Chem* 61, 3779-3798.
23. Dalkas, G. A., Marchand, D., Galleyrand, J. C., Martinez, J., Spyroulias, G. A., Cordopatis, P. and Cavelier, F. (2010) Study of a Lipophilic Captopril Analogue Binding to Angiotensin I Converting Enzyme. *J Pept Sci* 16, 91-97.
24. Cavelier, F., Marchand, D. and Martinez, J. (2008) α,α' -Disubstituted Amino Acids with Silylated Side Chains as Lipophilic Building Blocks for the Synthesis of Peptaibol Analogues. *Chem Biodivers* 5, 1279-1287.
25. Cavelier, F., Marchand, D., Martinez, J. and Sagan, S. (2004) Biological Activity of Silylated Amino Acid Containing Substance P Analogues. *J Pept Res* 63, 290-296.
26. Meanwell, N. A. (2011) Synopsis of Some Recent Tactical Application of Bioisosteres in Drug Design. *J Med Chem* 54, 2529-2591.

27. Pujals, S., Fernandez-Carneado, J., Kogan, M. J., Martinez, J., Cavelier, F. and Giralt, E. (2006) Replacement of a Proline with Silaproline Causes a 20-Fold Increase in the Cellular Uptake of a Pro-Rich Peptide. *J Am Chem Soc* 128, 8479-8483.
28. Rémond, E., Martin, C., Martinez, J. and Cavelier, F. (2016) Silicon-Containing Amino Acids: Synthetic Aspects, Conformational Studies, and Applications to Bioactive Peptides. *Chem Rev* 116, 11654-11684.
29. Rémond, E., Martin, C., Martinez, J. and Cavelier, F. (2017) Silaproline, a Silicon-Containing Proline Surrogate. *Top Heterocycl Chem* 48, 27-50.
30. Fanelli, R., Berthomieu, D., Didierjean, C., Doudouh, A., Lebrun, A., Martinez, J. and Cavelier, F. (2017) Hydrophobic α,α -Disubstituted Disilylated Tesdpg Induces Incipient 310-Helix in Short Tripeptide Sequence. *Org Lett* 19, 2937-2940.
31. Cavelier, F., Vivet, B., Martinez, J., Aubry, A., Didierjean, C., Vicherat, A. and Marraud, M. (2002) Influence of Silaproline on Peptide Conformation and Bioactivity. *J Am Chem Soc* 124, 2917-2923.
32. Fanelli, R., Besserer-Offroy, E., Rene, A., Cote, J., Tetreault, P., Collette-Tremblay, J., Longpre, J. M., Leduc, R., Martinez, J., Sarret, P. et al. (2015) Synthesis and Characterization in Vitro and in Vivo of (L)-(Trimethylsilyl)Alanine Containing Neurotensin Analogues. *J Med Chem* 58, 7785-7795.
33. Granier, C., Van Rietschoten, J., Kitabgi, P., Poustis, C. and Freychet, P. (1982) Synthesis and Characterization of Neurotensin Analogues for Structure/Activity Relationship Studies. *Eur. J. Biochem.* 124, 117-125.
34. St-Pierre, S., Lalonde, J. M., Gendreau, M., Quirion, R., Regoli, D. and Rioux, F. (1981) Synthesis of Peptides by the Solid-Phase Method. 6. Neurotensin, Fragments, and Analogues. *J Med Chem* 24, 370-376.
35. René, A., Vanthuyne, N., Martinez, J. and Cavelier, F. (2013) (L)-(Trimethylsilyl)Alanine Synthesis Exploiting Hydroxypinanone-Induced Diastereoselective Alkylation. *Amino Acids* 45, 301-307.
36. Morgat, C., Mishra, A. K., Varshney, R., Allard, M., Fernandez, P. and Hindie, E. (2014) Targeting Neuropeptide Receptors for Cancer Imaging and Therapy: Perspectives with Bombesin, Neurotensin, and Neuropeptide-Y Receptors. *J Nucl Med* 55, 1650-1657.
37. Herrmann, K., Schwaiger, M., Lewis, J. S., Solomon, S. B., McNeil, B. J., Baumann, M., Gambhir, S. S., Hricak, H. and Weissleder, R. (2020) Radiotheranostics: A Roadmap for Future Development. *Lancet Oncol* 21, e146-e156.
38. Mansi, R., Wang, X., Forrer, F., Waser, B., Cescato, R., Graham, K., Borkowski, S., Reubi, J. C. and Maecke, H. R. (2011) Development of a Potent DOTA-Conjugated Bombesin Antagonist for Targeting Grpr-Positive Tumours. *Eur J Nucl Med Mol Imaging* 38, 97-107.
39. Jia, Y., Zhang, W., Fan, W., Brusnahan, S. and Garrison, J. (2016) Investigation of the Biological Impact of Charge Distribution on a NTR₁-Targeted Peptide. *Bioconjug Chem* 27, 2658-2668.
40. Doulut, S., Rodriguez, M., Lugrin, D., Vecchini, F., Kitabgi, P., Aumelas, A. and Martinez, J. (1992) Reduced Peptide Bond Pseudopeptide Analogues of Neurotensin. *Pept Res* 5, 30-38.
41. Fanelli, R., Floquet, N., Besserer-Offroy, E., Delort, B., Vivancos, M., Longpré, J. M., Renault, P., Martinez, J., Sarret, P. and Cavelier, F. (2017) Use of Molecular Modeling to Design Selective NTS₂ Neurotensin Analogues. *J Med Chem* 60, 3303-3313.
42. Maschauer, S. and Prante, O. (2018) Radiopharmaceuticals for Imaging and Endoradiotherapy of Neurotensin Receptor-Positive Tumors. *J Labelled Comp Radiopharm* 61, 309-325.
43. Maschauer, S., Greff, C., Einsiedel, J., Ott, J., Tripal, P., Hubner, H., Gmeiner, P. and Prante, O. (2015) Improved Radiosynthesis and Preliminary in Vivo Evaluation of a ¹⁸F-Labeled Glycopeptide-Peptoid Hybrid for PET Imaging of Neurotensin Receptor 2. *Bioorg Med Chem* 23, 4026-4033.
44. Swift, S. L., Burns, J. E. and Maitland, N. J. (2010) Altered Expression of Neurotensin Receptors Is Associated with the Differentiation State of Prostate Cancer. *Cancer Res* 70, 347-356.
45. Hindie, E., Zanotti-Fregonara, P., Quinto, M. A., Morgat, C. and Champion, C. (2016) Dose Deposits from ⁹⁰Y, ¹⁷⁷Lu, ¹¹¹In, and ¹⁶¹Tb in Micrometastases of Various Sizes: Implications for Radiopharmaceutical Therapy. *J Nucl Med* 57, 759-764.
46. Champion, C., Quinto, M. A., Morgat, C., Zanotti-Fregonara, P. and Hindie, E. (2016) Comparison between Three Promising Beta-Emitting Radionuclides, ⁶⁷Cu, ⁴⁷Sc and ¹⁶¹Tb, with Emphasis on Doses Delivered to Minimal Residual Disease. *Theranostics* 6, 1611-1618.

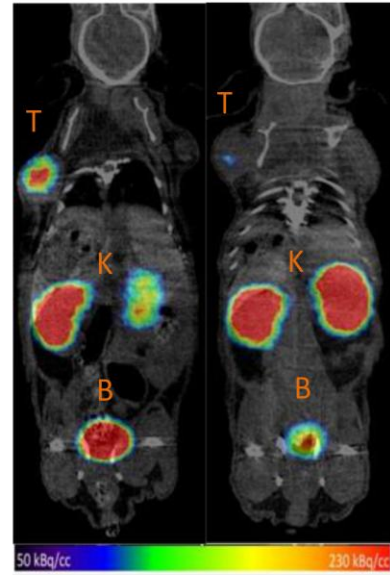
47. Kratochwil, C., Bruchertseifer, F., Giesel, F. L., Weis, M., Verburg, F. A., Mottaghy, F., Kopka, K., Apostolidis, C., Haberkorn, U. and Morgenstern, A. (2016) ^{225}Ac -PSMA-617 for PSMA-Targeted Alpha-Radiation Therapy of Metastatic Castration-Resistant Prostate Cancer. *J Nucl Med* 57, 1941-1944.
48. Muller, C., Umbricht, C. A., Gracheva, N., Tschan, V. J., Pellegrini, G., Bernhardt, P., Zeevaart, J. R., Koster, U., Schibli, R. and van der Meulen, N. P. (2019) Terbium-161 for PSMA-Targeted Radionuclide Therapy of Prostate Cancer. *Eur J Nucl Med Mol Imaging* 46, 1919-1930.
49. Baum, R. P., Singh, A., Schuchardt, C., Kulkarni, H. R., Klette, I., Wiessalla, S., Osterkamp, F., Reineke, U. and Smerling, C. (2018) ^{177}Lu -3BP-227 for Neurotensin Receptor 1-Targeted Therapy of Metastatic Pancreatic Adenocarcinoma: First Clinical Results. *J Nucl Med* 59, 809-814.
50. Misu, R., Noguchi, T., Ohno, H., Oishi, S. and Fujii, N. (2013) Structure-Activity Relationship Study of Tachykinin Peptides for the Development of Novel Neurokinin-3 Receptor Selective Agonists. *Bioorg Med Chem* 21, 2413-2417.
51. Lang, C., Maschauer, S., Hubner, H., Gmeiner, P. and Prante, O. (2013) Synthesis and Evaluation of a ^{18}F -Labeled Diarylpyrazole Glycoconjugate for the Imaging of NTS₁-Positive Tumors. *J Med Chem* 56, 9361-9365.
52. Teodoro, R., Faintuch, B. L., Nunez, E. G. and Queiroz, R. G. (2011) Neurotensin(8-13) Analogue: Radiolabeling and Biological Evaluation Using Different Chelators. *Nucl Med Biol* 38, 113-120.
53. Osterkamp, F., Smerling, C., Reineke, U., Hasse, C. and Ungewib, J. (2014) Neurotensin Receptor Ligands. WO 2014/086499
54. Bar-Shavit, Z. and Goldman, R. (1982) Tuftsin and Substance P as Modulators of Phagocyte Functions. *Adv Exp Med Biol* 141, 549-558.
55. Goldman, R., Bar-Shavit, Z. and Romeo, D. (1983) Neurotensin Modulates Human Neutrophil Locomotion and Phagocytic Capability. *FEBS Lett* 159, 63-67.
56. Saada, S., Marget, P., Fauchais, A. L., Lise, M. C., Chemin, G., Sindou, P., Martel, C., Delpy, L., Vidal, E., Jaccard, A., et al. (2012) Differential Expression of Neurotensin and Specific Receptors, NTSR₁ and NTSR₂, in Normal and Malignant Human B Lymphocytes. *J Immunol* 189, 5293-5303.
57. Benesova, M., Schafer, M., Bauder-Wust, U., Afshar-Oromieh, A., Kratochwil, C., Mier, W., Haberkorn, U., Kopka, K. and Eder, M. (2015) Preclinical Evaluation of a Tailor-Made DOTA-Conjugated PSMA Inhibitor with Optimized Linker Moiety for Imaging and Endoradiotherapy of Prostate Cancer. *J Nucl Med* 56, 914-920.
58. Schulz, J., Rohracker, M., Stiebler, M., Goldschmidt, J., Stober, F., Noriega, M., Pethe, A., Lukas, M., Osterkamp, F., Reineke, U., et al. (2017) Proof of Therapeutic Efficacy of a ^{177}Lu -Labeled Neurotensin Receptor 1 Antagonist in a Colon Carcinoma Xenograft Model. *J Nucl Med* 58, 936-941.
59. Afshar-Oromieh, A., Hetzheim, H., Kubler, W., Kratochwil, C., Giesel, F. L., Hope, T. A., Eder, M., Eisenhut, M., Kopka, K. and Haberkorn, U. (2016) Radiation Dosimetry of ^{68}Ga -PSMA-11 (Hbed-Cc) and Preliminary Evaluation of Optimal Imaging Timing. *Eur J Nucl Med Mol Imaging* 43, 1611-1620.
60. Sandstrom, M., Velikyan, I., Garske-Roman, U., Sorensen, J., Eriksson, B., Granberg, D., Lundqvist, H., Sundin, A. and Lubberink, M. (2013) Comparative Biodistribution and Radiation Dosimetry of ^{68}Ga -Dotatoc and ^{68}Ga -Dotatate in Patients with Neuroendocrine Tumors. *J Nucl Med* 54, 1755-1759.

TABLE OF CONTENTS GRAPHIC



↑ Uptake
 ↑ Stability
 ↑ Selectivity
 →

[68Ga]Ga-JMV6659 | Blocked



T = tumor; K = kidneys; B = bladder